



## Performance of New Absorber Coating Strategy in Solar Air Heaters: An Experimental Case Study

M. Mahmoudi<sup>1</sup>, H. Farzan<sup>1\*</sup>, E. Hasan Zaim<sup>2</sup>

<sup>1</sup> Mechanical Engineering Department, Higher Education Complex of Bam, Bam, Iran

<sup>2</sup> Mechanical Engineering Faculty, Sirjan University of Technology, Kerman, Iran

### PAPER INFO

#### Paper history:

Received 21 December 2021

Accepted in revised form 06 March 2022

#### Keywords:

Aluminum shavings  
Asphalt solar air heater  
Coating strategy  
Heat dynamics  
Thermal performance

### ABSTRACT

Asphalt materials commonly have high absorption coefficients, and their surface temperature reaches as high as 80 °C during daytime hours since their surfaces are exposed to solar radiation for long periods. Hence, asphalt pavements can easily be converted to solar air heaters (SAHs) to collect solar energy. Even though asphalt materials have low thermal conductivity, resulting in a weak convection heat exchange rate between the flowing air and asphalt surface. The current experimental study analyzes utilizing aluminum shavings as asphalt coating materials to improve SAHs' thermal performance. To this aim, a serpentine SAH prototype was constructed, and several sensors were utilized to monitor its dynamic thermal response. Black-painted aluminum shavings were utilized as coating materials to improve the convective heat exchange rate and increase the roughness of the absorber surface. Two scenarios were considered, including the uncoated absorber plate and coated one with 0.2 kg aluminum shavings. The experiments were carried out for two air mass flow rates of 0.02 kg/s and 0.03 kg/s under field conditions. Based on the air mass flow rate, the coated absorber reaches higher temperatures, approximately 5 °C to 9 °C, than the uncoated one. The acquired results illustrate that the coated SAH has nearly 4 °C to 5 °C higher maximum exhaust air temperature; hence, the coating strategy improves the thermal efficiency by 24.75% and 44% in two air mass flow rates of 0.02 kg/s and 0.03 kg/s, respectively.

doi: 10.5829/ijee.2022.13.02.03

### NOMENCLATURE

$A_c$	collector area, m <sup>2</sup>	$I$	incoming
$c_p$	specific heat, J/kg. K	$in$	inlet
$G$	solar irradiation heat flux, W/m <sup>2</sup>	$out$	outlet
$\dot{m}$	mass flow rate, kg/s	$U$	useful
$P$	pressure, Pa	$S$	stored
$Q$	energy, J	<b>Greek Symbols</b>	
$T$	temperature, °C	$\eta$	efficiency
$v$	air velocity, m/s	$\omega$	uncertainty

### Subscripts

$a$  air

### INTRODUCTION

Solar energy is the most affordable renewable energy that has been extensively used to produce green thermal

energy. Numerous techniques have been introduced to harvest solar thermal energy, and SAHs are the most affordable and simple collectors among these techniques [1, 2]. These collectors utilize varieties of heat absorbers

\*Corresponding Author Email: [hadi.farzan@bam.ac.ir](mailto:hadi.farzan@bam.ac.ir) (H. Farzan)

to accumulate incoming solar energy. Pavements are exposed to solar radiation for a long time during daytime hours, and their surface temperature can reach nearly to 80 °C; hence, pavements can serve as affordable heat absorbers [3]. Pavements are accessible infrastructure everywhere and cheap; however, pavements as heat absorbers have a critical drawback in which pavement materials inherently have a low thermal conductivity. This issue affects the heat dynamics of SAHs and reduces thermal performance.

Numerous literature investigated SAHs' performance due to their simple structure, easy construction and maintenance, and low-cost operation [4, 5]. These studies assessed simple, effective, and affordable techniques such as artificial roughness, corrugations, and coating strategies to improve the performance of solar air heaters [6, 7]. El-Sebaei and Al-Snani [8] analyzed the performance of solar air heaters using absorber plates coated with numerous selective coating materials. They illustrated that the optimum performance was obtained by utilizing nickel-tin with 46% daily efficiency. Zhang et al. [9] reviewed the aging mechanisms and thermal stability of absorber coatings. Malliga and Rajasekhar [10] investigated baffle-arranged absorbers coated with nano graphite and CuO. Using this technique, they reported that the maximum working fluid temperature reached to 59.4 °C. Arunkumar et al. [11] used nanostructured CuO as coating materials in a solar still to improve thermal performance by 5%. A comparison between a conventional SAH and a SAH using artificial roughness and absorber coating materials illustrated that the equipped SAH had higher performance and outlet temperature around 7.5% and 13.5 °C, respectively. Abdelkader et al. [12, 13] used CNTs/CuO black paint as coating materials in a flat plate solar air heater using ribs roughness. Using these methods caused thermal performance to increase by 18.8% compared to a conventional SAH. Das et al. [14] investigated the heat dynamics of a sand-filled SAH and compared the results with a SAH using an aluminum absorber. The used sands simultaneously acted as coating and thermal storage units and improved performance by nearly 39% higher performance than the SAH using the aluminum absorber.

Extensive research emphasized utilizing artificial roughness and corrugations to boost the thermal performance of SAHs [15, 16]. Sebaei et al. [17] illustrated that adding corrugations to absorber plates in flat plate SAHs could improve their thermal efficiency by 11-14%. Sebaei et al. [18] extended their research study to assess the efficiencies of V-corrugated solar air heaters. The experimental results illustrated that the double pass V-corrugated plate SAH had 9.3-11.9% higher efficiency than the double-pass-finned SAH. An experimental study indicated the thermal efficiency of a double-pass SAH with 2, 4, and 6 fins attached at the same mass flow rate was 75%, 82.1%, and 85.9%, respectively [19]. Some literature investigated the exergetic and energetic

performance of SAHs using different types of extended surfaces and baffles [20]. The acquired results proved that increasing the artificial roughness improves the SAHs thermal performance at low mass flow rates, but the exergetic performance significantly reduces at high mass flow rates. Ravi and Saini [21] and Alam and Kim [22] assessed the efficiency enhancement methods of SAHs, such as using phase change materials, artificial roughness, and corrugated/grooved absorbing surfaces. These performance enhancement techniques were assessed and discussed in detail through literature [23-28]. Kumar and Chand [29], Kumar and Layek [30], and Kabeel et al. [31] determined the effects of fin spacing ratio, fin pitch, and fin height on the efficiency of solar air collectors. The analytical results showed that SAH's thermal efficiency could increase by 80.1% using this approach. Using the roughness and turbulator was extensively employed to improve the exergetic and energetic thermal performance, while numerical or analytical methods were employed to optimize the roughness parameters [32-34]. Gholami et al. [35] performed a thermo-economic optimization of a single pass solar air heater with artificial roughness based on the exergy efficiency.

As discussed in the current literature, numerous studies investigated the performance of SAHs using techniques such as corrugations and selective coating materials to improve the performance of SAHs. The assessed absorbers in these studies are metals made of stainless steel and aluminum sheets. However, due to high conductivity utilizing metallic absorbers improves the thermal performance of SAHs, but they are expensive and costly to be machined. On the other hand, Pavements are easily accessible infrastructure that can be easily converted into low-cost absorbers. The current study investigates the dynamic thermal response and performance of finned SAHs with asphalt pavements serving as absorber plates. To achieve this goal, a SAH with staggered fin arrays was constructed, and the pavement surface was coated with black-painted aluminum shavings to add roughness to the absorber surface while also improving absorber conductivity. Two chief aims of the current study are assessing asphalt pavements' capability to use as absorber plates and evaluating aluminum shavings' effectiveness in thermal performance improvement. The experimental runs were carried out in two air mass flow rates under field conditions while several sensors were utilized to simultaneously monitor the dynamic thermal response of the SAH and environmental conditions.

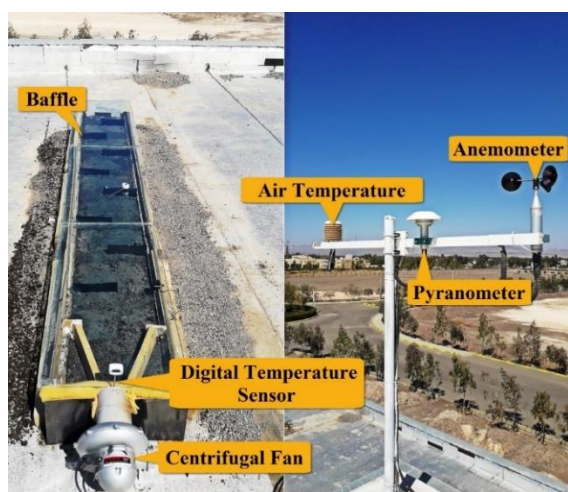
Asphalt materials have a low thermal conductivity and heat diffusion, affecting the efficiency of SAHs. The current study suggests a technique to address this problem, in which the asphalt surface is coated with black-painted aluminum shavings to improve the heat exchange between the flowing air and asphalt materials. Two scenarios were considered to experimentally

investigate the importance of using aluminum shavings on the asphalt absorber plate, including uncoated asphalt pavement and asphalt pavement coated with 0.2 kg aluminum shavings.

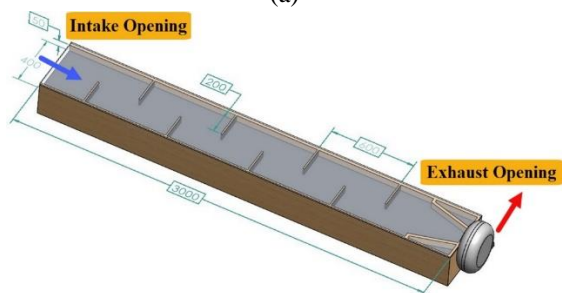
## MATERIAL AND METHODS

### Experimental setup

The constructed experimental setup is shown in Figure 1. The designed asphalt SAH is constructed of a wooden box filled with asphalt materials. The asphalt materials serve as the heat absorber, gaining solar energy and heating flowing air. The asphalt surface was compacted with a compactor to minimize air void content in the used asphalt mixture.



(a)



(b)



(c)

**Figure 1.** (a) Constructed experimental setup, (b) its dimensions in mm, and (c) aluminum shavings.

Several stainless-steel baffles were used on the absorber surface to produce a serpentine air passageway and improve the convective heat transfer mechanism. A 10 mm thick glass plate was installed 40 mm above the absorber to protect it and decrease convective/radiant heat losses to ambient environments. The critical experimental setup component and their technical specifications are given in Table 1. A convergent duct at the exhaust opening helps the airflow leave the SAH uniformly. A centrifugal air blower sucks cold air into the collector and exhausts hot air to the ambient, and all voids and seams were sealed with silicone sealants to avoid air leakage.

### Absorber coating strategies

Material, configuration, and coating of absorber plates have a crucial role in the thermal efficiency of SAHs. Asphalt pavements are accessible infrastructures exposed to solar irradiation log time a day; hence they have a significant potential to use as absorber plates. However, asphalt pavements have a low thermal conductivity, and this issue reduces the heat exchange between the airflow and absorber. This study evaluates the dynamic thermal response of SAHs using asphalt pavements as heat absorbers. Two coating strategies were considered and assessed to obtain the impacts of absorber coating on the dynamic thermal response and thermal efficiency of asphalt SAHs. Two scenarios were analyzed, including uncoated asphalt pavement and coated asphalt pavement with 0.2 kg aluminum shavings. Table 2 represents the thermophysical properties of aluminum and asphalt materials.

**Table 1.** Critical asphalt SAH component and technical specifications

Component	Specification	Value
Framework	Material	Russian wood
	Length	3000 mm
	Width	400 mm
	Height	200 mm
Heat absorber	Material	Asphalt materials (Bitumen 60/70)
Baffle	Material	Stainless steel
	Number	Seven
	Length	200 mm
	Width	50 mm
	Thickness	5 mm
Glazing	Material	Low iron glass
	Thickness	10 mm
Air blower type	Centrifugal fan	120 Watts

**Table 2.** Thermal properties of heat absorber and coating materials

Component	$k$ (W/m.K)	$c_p$ (J/kg.K)	$\rho$ (kg/m <sup>3</sup> )	$\epsilon$
Asphalt Material [36-39]	1.0	1485	2450	0.95
Aluminum	225.94	921	2698	N.A.

The aluminum was selected to serve as the asphalt pavement coating due to its high thermal conductivity, strength, and availability. The utilized aluminum shavings were painted in black color and homogeneously dispersed on the pavement top surface. These shavings were produced by machining processing and had a maximum particle size of 1 mm.

**Measurement**

Several sensors were employed to monitor critical environmental factors and temperatures that determine the dynamic thermal response of the collector. These factors include the intake/exhaust air temperature, asphalt surface temperature, ambient temperature, and solar irradiation. The Thermo TA-288 digital thermometers measured the inlet/outlet air and asphalt surface temperatures. Environmental conditions, including ambient air temperature, and solar irradiation, were measured with sensors installed on the weather station. The Kipp&Zonen CMP3 pyranometer measured solar irradiation, and the Parto Negar TH202-485 thermometer and TROTEC BA06 attained the ambient air temperature and airflow velocity.

**Test conditions**

The experiments were carried out in the Higher Education Complex of Bam, Bam, Iran (29° 6' N, 58° 21' E, 1061 m above sea level). Bam has long, sweltering, arid summers and cold, dry, and mostly clear winters. Over the year, the temperature typically varies from 5 °C to 39 °C and is rarely below 0 °C or above 42 °C.

The experimental tests began at 9:00 A.M. and ended at 3:00 P.M. for 6 hours under field conditions through autumn 2021. The weather was clear and sunny during the experimental runs. The installed blower ran to produce a continuous airflow at two different flow rates of 0.02 kg/s and 0.03 kg/s. The airflow rate was set by adjusting the variable intake vane. The critical measured temperatures and environmental factors were recorded in every 15 min to analyze the collector’s dynamics.

**Uncertainty analysis**

Uncertainty analysis aims to determine how the experimental data were accurately collected and the obtained data were reliable. Numerous factors, including methodology, experimental conditions, and instrumentation, affect data accuracy and reliability. The

current study attempted to utilize accurate and precise instruments to measure the crucial parameters such as inlet and outlet air temperatures. The accuracy and uncertainty of the main measured factors are represented in Table 3.

These measured factors were used to compute air mass flow rate, heat gain, and daily thermal efficiency. The uncertainties associated with these parameters were obtained using Kline’s method [40].

$$\frac{\omega_{\dot{m}_a}}{\dot{m}_a} = \left[ \left( \frac{\omega_{T_a}}{T_a} \right)^2 + \left( \frac{\omega_{v_{in}}}{v_{in}} \right)^2 + \left( \frac{\omega_{P_a}}{P_a} \right)^2 \right]^{\frac{1}{2}} \tag{1a}$$

$$\frac{\omega_Q}{Q} = \left[ \left( \frac{\omega_{\dot{m}_a}}{\dot{m}_a} \right)^2 + \left( \frac{\omega_{\Delta T}}{\Delta T} \right)^2 \right]^{\frac{1}{2}} \tag{1b}$$

$$\frac{\omega_{\eta}}{\eta_{Daily}} = \left[ \left( \frac{\omega_{\dot{m}_a}}{\dot{m}_a} \right)^2 + \left( \frac{\omega_{\Delta T}}{\Delta T} \right)^2 + \left( \frac{\omega_G}{G} \right)^2 \right]^{\frac{1}{2}} \tag{1c}$$

Here  $\omega$  denotes the uncertainty.  $\dot{m}_a$ ,  $T_a$ , and  $v_{in}$  are the air mass flow rate, ambient air temperature, and intake air velocity, respectively.  $\Delta T$  represents the air temperature difference at the collector openings, and  $G$  is the measured solar irradiation. Using Kline’s method, the calculated uncertainties for the air mass flow rate, heat gain, and daily thermal efficiency are 3.5%, 2.4%, and 4.1%, respectively.

**Energy analysis**

Energy analysis assesses and compares the performance of energy systems and provides insights into performance improvement. The energy balance equations can be utilized to carry out the energy analysis. According to the energy balance equations in the constructed asphalt SAH, we have:

$$Q_i = Q_U + Q_S + Q_L \tag{2}$$

**Table 3.** The accuracy and uncertainty of main parameters

Parameter	Accuracy	Uncertainty
Intake Air Temperature	0.5 °C	5%
Exhaust Air Temperature	0.5 °C	5%
Airflow Velocity	0.3 m/s	3%
Ambient Air Temperature	0.5 °C	5%
Solar Irradiation	10 W/m <sup>2</sup>	3%
Wind Velocity	0.01 m/s	5%

Here  $Q_I$ ,  $Q_U$ ,  $Q_S$ ,  $Q_L$  are the incoming, useful, stored, and lost energy. The daily incoming solar energy that hits the collector is given as follows.

$$Q_I = A_c \int_{t_1}^{t_2} G dt \quad (3)$$

While the useful heat gain by the collector is defined as follows.

$$Q_U = \dot{m}_a c_p \int_{t_1}^{t_2} (T_{a,ex} - T_{a,in}) dt \quad (4)$$

Here  $\dot{m}_a$  is the air mass flow rate.  $T_{a,in}$  and  $T_{a,out}$  show the intake and exhaust air temperatures, respectively.  $A_c$  is the collector surface area. Based on the first law efficiency, the daily thermal efficiency is defined as the ratio of the total heat gain divided by the total incoming solar energy.

$$\eta_{Daily} = \frac{Q_U}{Q_I} \quad (5)$$

**RESULTS AND DISCUSSION**

Since ambient conditions such as outdoor temperature and solar irradiation have a significant impact on the dynamic thermal response of the collector, they were monitored and measured over the course of the experiments using precise sensors. The input energy is determined by solar irradiation, while the outdoor temperature specifies the intake temperature and heat losses to the ambient environment. In other words, the higher the temperature difference between the absorber and the ambient temperature, the greater the heat losses to the surrounding environment. The measured environmental parameters are depicted in Figure 2. During the experimental runs from 9:00 A.M. to 3:00 P.M., the solar intensity varied from 180 W/m<sup>2</sup> to 560 W/m<sup>2</sup>, while the outdoor temperature increased from 10°C to nearly 21°C. The solar intensity is low in the early morning and late in the evening, resulting in insufficient solar energy hitting the absorber plate.

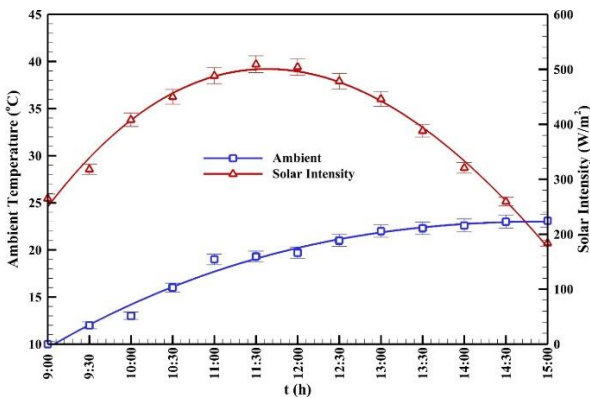
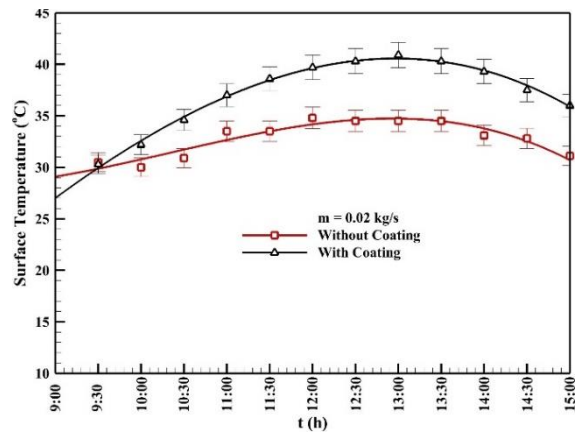


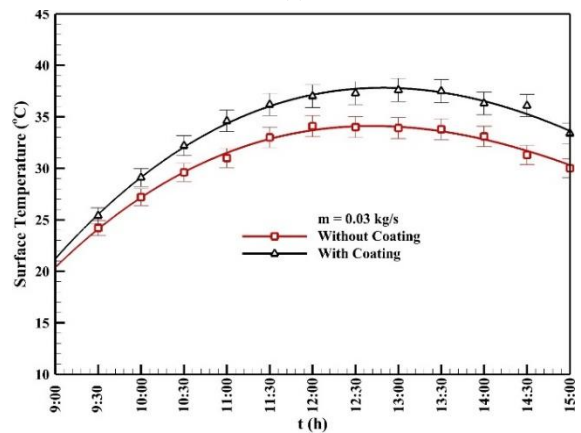
**Figure 2.** Measured ambient conditions

Figures 3a and 3b show the absorber surface temperature in two considered scenarios. The absorber surface temperature defines the maximum possible temperature that the exhaust temperature can achieve. As shown in Figures 3a and 3b, the coated absorber has a higher temperature than the uncoated absorber. Using the coating strategy increases the maximum absorber plate temperature by 9 °C and 5 °C in two air mass flow rates of 0.02 kg/s and 0.03 kg/s. This issue illustrates that the used coating strategy effectively increases the absorber plate temperature and, consequently, maximum potential exhaust air temperature. Furthermore, the absorber surface temperature is a function of incoming solar radiation, and its profile has the same trend as the solar intensity. Hence, the higher the absorbed solar energy, the higher the absorber plate temperature.

As illustrated in Figures 3a and 3b, mass flow rate significantly affects the absorber plate temperature. The convective heat exchange rate between the flowing air and the absorber plate improves in the constructed SAH by increasing the air mass flow rate. Hence, the higher thermal energy exchanges between the cold flowing air



(a)



(b)

**Figure 3.** Surface tempertaure in two air mass flow rates (a) 0.02 kg/s and (b) 0.03 kg/s.

and the hot absorber plate. Therefore, the absorber plate experiences a lower temperature in the higher air mass flow rate of 0.03 kg/s. Figures 4a and 4b represent the exhaust air temperature measured by the digital sensor installed at the exhaust opening. The outdoor air was sucked into the collector by the installed fan, heated by the hot absorber plate, and then left the SAH. As shown in Figures. 4a and 4b, the intake air is cold at the beginning of the experimental runs, but its temperature increases due to heat exchange by the absorber plate. Interestingly, the solar intensity is low at 9:00 A.M., but the absorber plate is hot enough to increase the intake temperature averagely by 16 °C at the beginning of the experimental runs in all scenarios. This issue proves that asphalt materials have a great potential to serve as an absorber plate.

The exhaust temperature in the scenario using the coating strategy is higher than the scenario without using the coated absorber. In the scenario with the coated absorber, the absorber plate has a higher temperature due to using the black-painted aluminum shavings that

improve absorbing solar energy; furthermore, the coated absorber plate has a rougher surface than the uncoated surface. The rougher absorber plate improves the convective heat transfer between the absorber plate and the flowing air. Therefore, these issues result in the exhaust temperature experiencing higher temperatures when the coated absorber plate is used. The exhaust temperature in the SAH with coated absorber plate is averagely 5 °C to 6 °C higher than the scenario without using the coating.

Figures 4a and 4b proved that by increasing the air mass flow rate decreases the time air travels inside the collector; however, the convective heat transfer coefficient increases due to higher air velocity inside the SAH. These two factors have the opposite effect. However, the acquired result proves that the air leaves the collector at a lower temperature when the air mass flow rate increases from 0.02 kg/s to 0.03 kg/s.

Figure 5 (a, b) represents the calculated temperature difference during the experiments. The temperature difference determines the heat gain, and consequently, the

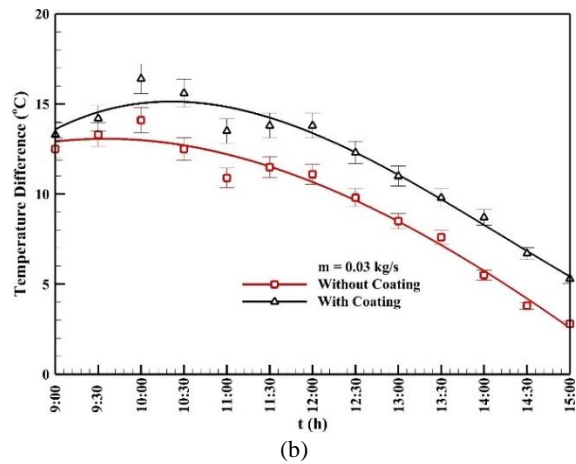
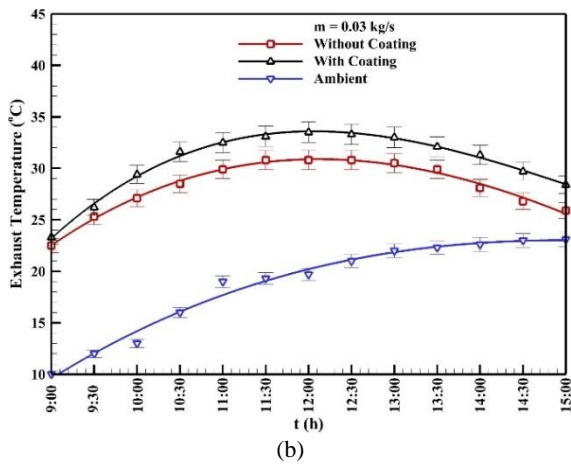
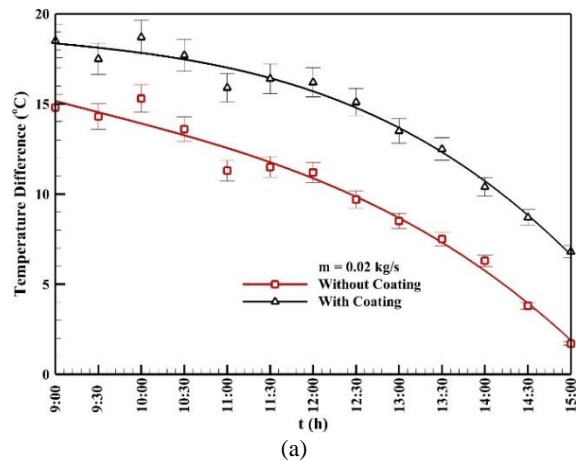
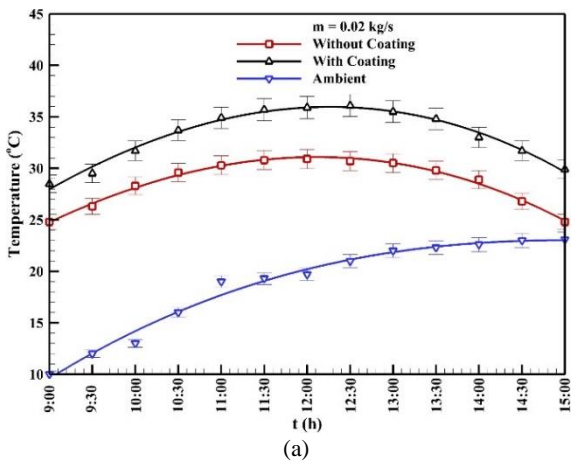


**Figure 4.** Measured exhaust air temperature in two air mass flow rates (a) 0.02 kg/s and (b) 0.03 kg/s.

**Figure 5.** Calculated temperature difference in two air mass flow rates (a) 0.02 kg/s and (b) 0.03 kg/s.

thermal performance of the constructed SAH. The temperature difference reduces from the beginning to the end of the experiments. Indeed, the intake temperature grows from 10 °C to 20 °C during the experimental runs; furthermore, the solar intensity decreases significantly in the evening. These factors cause the temperature difference to decrease from the beginning to the end of the test in the evening.

The temperature difference profiles have the same approach as the exhaust and surface temperature profiles. The coated strategy increases the temperature difference, resulting in increasing the accumulated heat gain.

Figure 6 shows the calculated heat gains in all scenarios in each hour during the experiments. Figure 6 shows that using the coated absorber plate and increasing the mass flow rate enhance the accumulated heat gain in all scenarios considered. In the evening, when the solar intensity is low, the accumulated heat gains in the scenarios with the uncoated absorber plate are significantly lower than in the scenario with the coated absorber. Using the coating strategy helps the absorber plate fasten discharging its heat content when the solar intensity and absorber temperature are low. Furthermore, in the morning, the difference between the accumulated heat gains in the coated scenario is more pronounced than in the uncoated scenario for the mass flow rates of 0.02

kg/s and 0.03 kg/s. The coating strategy improves the charge/discharge process in the SAH. The heat gains in the scenario using the coating strategy are 18.873 MJ and 34.133 MJ for the air mass flow rates of 0.02 kg/s and 0.03 kg/s, respectively, while the SAH without coated absorber plate gains 15.124 MJ and 23.661 MJ for two considered mass flow rates. As illustrated, coating the absorber plate increases the accumulated heat gain by 24.8% and 44.2% for the air mass flow rates of 0.02 kg/s and 0.03 kg/s, respectively.

Table 4 shows the calculated daily thermal efficiency in two scenarios considered. Computing and comparing the thermal efficiency are robust approaches to analyze energy systems using different technologies or approaches. As shown in Table 4, the SAH with the coated absorber plate has higher daily thermal efficiency, and by increasing the air mass flow rate, the daily thermal efficiency also improves. The daily thermal efficiency in the scenario using the coating strategy reaches 30.4% in the mass flow rate of 0.03 kg/s, while the SAH with the uncoated absorber has the maximum efficiency of 21.1% in the same air mass flow rate.

**Table 4.** Calculated daily thermal efficiency

Scenario	Thermal Efficiency	
	0.02 kg/s	0.03 kg/s
Uncoated	20.2%	21.1%
Coated	25.2%	30.4%

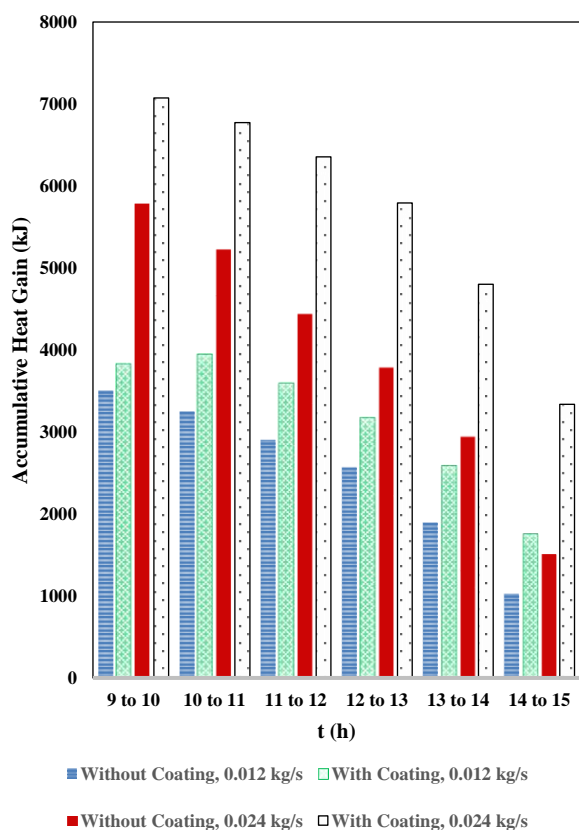


**Figure 6.** Accumulated heat gains in different scenarios

## CONCLUSION

Increasing the thermal efficiency of SAHs is a goal of many studies, and several techniques have been developed to achieve this aim. The current study assesses an affordable technique that many collectors can easily use. This technique proposes using aluminum shavings as an absorber coating to absorb more incoming solar energy. To this aim, an asphalt SAH was constructed, and its dynamic thermal response was monitored in two scenarios, including uncoated and coated absorber plate by aluminum shavings. The acquired results illustrated that:

- Using aluminium shavings increases the absorber temperature during the experimental runs by nearly 7 °C to 5 °C for the air mass flow rates of 0.02 kg/s and 0.03 kg/s.
- Increasing the absorber temperature enhances the exhaust temperature. The coating strategy increases the exhaust temperature by nearly 5 °C to 3 °C for the air mass flow rates of 0.02 kg/s and 0.03 kg/s.
- Since the coated strategy increases the exhaust temperature, consequently the accumulated heat gains improve.

- The accumulated heat gains in the scenarios using the coating strategy are 24.8% and 44.2% are higher than those without the coating strategy for the air mass flow rates of 0.02 kg/s and 0.03 kg/s, respectively.
- The higher the accumulated heat gain, the higher the thermal performance. The daily thermal efficiency of the SAH with coated absorber plate reaches 30.4%, while the same collector without coated absorber has a daily thermal efficiency of 21.1%.
- The acquired results illustrate that using the coating strategy is a robust and affordable approach to improving accumulated heat gain and daily thermal efficiency.
- The air mass flow affects the dynamic thermal response of the SAH. Increasing the air mass flow rate improves daily thermal efficiency. However, it decreases the maximum exhaust temperature in all scenarios considered.

## ACKNOWLEDGEMENT

The authors would like to thank the Higher Education Complex of Bam and Sirjan University of Technology for their supports.

## REFERENCES

- Nnamchi, S., Nnamchi, O., Sangotayo, E., Ismael, S., Nkurunziza, O. and Gabriel, V., 2020. "Design and simulation of air-solar preheating unit: An improved design of a flat plate solar collector". *Iranian (Iranica) Journal of Energy & Environment*, 11(2), pp.97-108. Doi: 10.5829/ijee.2020.11.02.02
- Gandjalikhan Nassab, S. and Moein Addini, M., 2021. "Performance augmentation of solar air heater for space heating using a flexible flapping guide winglet". *Iranian (Iranica) Journal of Energy & Environment*, 12(2), pp.161-172. Doi: 10.5829/ijee.2021.12.02.09
- Farzan, H., Ameri, M. and Jaafarian, S., 2020. "Effectiveness of continuous and discontinuous-flow strategies in heat dynamics and performance of asphalt solar collector: An experimental study". *Iranian (Iranica) Journal of Energy & Environment*, 11(2), pp.137-145. Doi: 10.5829/ijee.2020.11.02.07
- Zhu, J., Jia, H., Cheng, X., Huang, X., Liu, X. and Guo, J., 2019. "The design and performance evaluation of a high-efficient flexible solar air heater based on transparent spacer fabric composite". *Solar Energy Materials and Solar Cells*, 201, pp.110089. Doi: 10.1016/j.solmat.2019.110089
- Ameri, M., Farzan, H. and Nobari, M., 2021. "Evaluation of different glazing materials, strategies, and configurations in flat plate collectors using glass and acrylic covers: An experimental assessment". *Iranian (Iranica) Journal of Energy & Environment*, 12(4), pp.297-306. Doi: 10.5829/ijee.2021.12.04.03
- Sakhaei, S.A. and Valipour, M.S., 2019. "Performance enhancement analysis of the flat plate collectors: A comprehensive review". *Renewable and Sustainable Energy Reviews*, 102, pp.186-204. Doi: 10.1016/j.rser.2018.11.014
- Rai, S., Chand, P. and Sharma, S., 2016. "Investigation of an offset finned solar air heater based on energy and exergy performance". *Iranian (Iranica) Journal of Energy & Environment*, 7(3), pp.212-220. Doi: 10.5829/idosi.ijee.2016.07.03.01
- El-Sebaai, A. and Al-Snani, H., 2010. "Effect of selective coating on thermal performance of flat plate solar air heaters". *Energy*, 35(4), pp.1820-1828. Doi: 10.1016/j.energy.2009.12.037
- Zhang, K., Hao, L., Du, M., Mi, J., Wang, J.-N. and Meng, J.-p., 2017. "A review on thermal stability and high temperature induced ageing mechanisms of solar absorber coatings". *Renewable and Sustainable Energy Reviews*, 67, pp.1282-1299. Doi: 10.1016/j.rser.2016.09.083
- Malliga, T.V. and Rajasekhar, R.J., 2017. "Preparation and characterization of nanographite-and cuo-based absorber and performance evaluation of solar air-heating collector". *Journal of Thermal Analysis and Calorimetry*, 129(1), pp.233-240. Doi: 10.1007/s10973-017-6155-1
- Arunkumar, T., Murugesan, D., Raj, K., Denkenberger, D., Viswanathan, C., Rufuss, D.D.W. and Velraj, R., 2019. "Effect of nano-coated CuO absorbers with PVA sponges in solar water desalting system". *Applied Thermal Engineering*, 148, pp.1416-1424. Doi:10.1016/j.applthermaleng.2018.10.129
- Abdelkader, T.K., Zhang, Y., Gaballah, E.S., Wang, S., Wan, Q. and Fan, Q., 2020. "Energy and exergy analysis of a flat-plate solar air heater coated with carbon nanotubes and cupric oxide nanoparticles embedded in black paint". *Journal of Cleaner Production*, 250, pp.119501. Doi: 10.1016/j.jclepro.2019.119501
- Abdelkader, T.K., Fan, Q., Gaballah, E.S., Wang, S. and Zhang, Y., 2020. "Energy and exergy analysis of a flat-plate solar air heater artificially roughened and coated with a novel solar selective coating". *Energies*, 13(4), pp.997. Doi:10.1016/j.jclepro.2019.119501
- Das, B., Mondol, J.D., Negi, S., Smyth, M. and Pugsley, A., 2020. "Experimental performance analysis of a novel sand coated and sand filled polycarbonate sheet based solar air collector". *Renewable Energy*, 164, pp.990-1004. Doi: 10.1016/j.renene.2020.10.054
- Akpınar, E.K. and Koçyiğit, F., 2010. "Energy and exergy analysis of a new flat-plate solar air heater having different obstacles on absorber plates". *Applied Energy*, 87(11), pp.3438-3450. Doi: 10.1016/j.apenergy.2010.05.017
- Ho, C.-D., Chang, H., Wang, R.-C. and Lin, C.-S., 2012. "Performance improvement of a double-pass solar air heater with fins and baffles under recycling operation". *Applied Energy*, 100, pp.155-163. Doi: 10.1016/j.apenergy.2012.03.065
- El-Sebaai, A., Aboul-Enein, S., Ramadan, M., Shalaby, S. and Moharram, B., 2011. "Investigation of thermal performance of double pass-flat and v-corrugated plate solar air heaters". *Energy*, 36(2), pp.1076-1086. Doi: 10.1016/j.energy.2010.11.042
- El-Sebaai, A., Aboul-Enein, S., Ramadan, M., Shalaby, S. and Moharram, B., 2011. "Thermal performance investigation of double pass-finned plate solar air heater". *Applied Energy*, 88(5), pp.1727-1739. Doi: 10.1016/j.apenergy.2010.11.017
- El-Khawajah, M., Aldabbagh, L. and Egelioglu, F., 2011. "The effect of using transverse fins on a double pass flow solar air heater using wire mesh as an absorber". *Solar Energy*, 85(7), pp.1479-1487. Doi: 10.1016/j.solener.2011.04.004
- Alta, D., Bilgili, E., Ertekin, C. and Yaldiz, O., 2010. "Experimental investigation of three different solar air heaters: Energy and exergy analyses". *Applied Energy*, 87(10), pp.2953-2973. Doi: 10.1016/j.apenergy.2010.04.016
- Ravi, R.K. and Saini, R.P., 2016. "A review on different techniques used for performance enhancement of double pass solar air heaters". *Renewable Sustainable Energy Reviews*, 56, pp.941-952. Doi: 10.1016/j.rser.2015.12.004
- Alam, T. and Kim, M.-H., 2017. "Performance improvement of double-pass solar air heater—a state of art of review". *Renewable Sustainable Energy Reviews*, 79, pp.779-793. Doi: 10.1016/j.rser.2017.05.087



23. Mahmood, A., Aldabbagh, L. and Egelioglu, F., 2015. "Investigation of single and double pass solar air heater with transverse fins and a package wire mesh layer". *Energy Conversion Management*, 89, pp.599-607. Doi: 10.1016/j.enconman.2014.10.028
24. Nowzari, R., Mirzaei, N. and Aldabbagh, L., 2015. "Finding the best configuration for a solar air heater by design and analysis of experiment". *Energy Conversion Management*, 100, pp.131-137. Doi: 10.1016/j.enconman.2015.04.058
25. Vaziri, R., İlkan, M. and Egelioglu, F., 2015. "Experimental performance of perforated glazed solar air heaters and unglazed transpired solar air heater". *Solar Energy*, 119, pp.251-260. Doi: 10.1016/j.solener.2015.06.043
26. Sahu, M.K. and Prasad, R.K., 2016. "Exergy based performance evaluation of solar air heater with arc-shaped wire roughened absorber plate". *Renewable Energy*, 96, pp.233-243. Doi:10.1016/j.renene.2016.04.083
27. Ravi, R.K. and Saini, R., 2018. "Effect of roughness elements on thermal and thermohydraulic performance of double pass solar air heater duct having discrete multi v-shaped and staggered rib roughness on both sides of the absorber plate". *Experimental Heat Transfer*, 31(1), pp.47-67. Doi: 10.1080/08916152.2017.1350217
28. Priyam, A. and Chand, P., 2018. "Effect of wavelength and amplitude on the performance of wavy finned absorber solar air heater". *Renewable Energy*, 119, pp.690-702. Doi: 10.1016/j.renene.2017.12.010
29. Kumar, R. and Chand, P., 2017. "Performance enhancement of solar air heater using herringbone corrugated fins". *Energy*, 127, pp.271-279. Doi: 10.1016/j.energy.2017.03.128
30. Kumar, A. and Layek, A., 2019. "Energetic and exergetic performance evaluation of solar air heater with twisted rib roughness on absorber plate". *Journal of Cleaner Production*, 232, pp.617-628. Doi: 10.1016/j.jclepro.2019.05.363
31. Kabeel, A., Hamed, M.H., Omara, Z. and Kandeal, A., 2018. "Influence of fin height on the performance of a glazed and bladed entrance single-pass solar air heater". *Renewable Solar Energy*, 162, pp.410-419. Doi: 10.1016/j.solener.2018.01.037
32. Singh, S., 2020. "Experimental and numerical investigations of a single and double pass porous serpentine wavy wiremesh packed bed solar air heater". *Renewable Energy*, 145, pp.1361-1387. Doi: 10.1016/j.renene.2019.06.137
33. Singh, S., Singh, A. and Chander, S., 2019. "Thermal performance of a fully developed serpentine wavy channel solar air heater". *Journal of Energy Storage*, 25, pp.100896. Doi: 10.1016/j.est.2019.100896
34. Afshari, F., Sözen, A., Khanlari, A., Tuncer, A.D. and Şirin, C., 2020. "Effect of turbulator modifications on the thermal performance of cost-effective alternative solar air heater". *Renewable Energy*, 158, pp.297-310. Doi: 10.1016/j.renene.2020.05.148
35. Gholami, A., Ajabshirchi, Y. and Ranjbar, S.F., 2019. "Thermoeconomic optimization of solar air heaters with arcuate-shaped obstacles". *Journal of Thermal Analysis Calorimetry*, 138(2), pp.1395-1403. Doi: 10.1007/s10973-019-08273-x
36. Luca, J. and Mrawira, D., 2005. "New measurement of thermal properties of superpave asphalt concrete". *Journal of Materials in Civil Engineering*, 17(1), pp.72-79. Doi: 10.1061/(ASCE)0899-1561(2005)17:1(72)
37. Yavuzturk, C., Ksaibati, K. and Chiasson, A., 2005. "Assessment of temperature fluctuations in asphalt pavements due to thermal environmental conditions using a two-dimensional, transient finite-difference approach". *Journal of Materials in Civil Engineering*, 17(4), pp.465-475. Doi: 10.1061/(ASCE)0899-1561(2005)17:4(465)
38. Gui, J., Phelan, P.E., Kaloush, K.E. and Golden, J.S., 2007. "Impact of pavement thermophysical properties on surface temperatures". *Journal of Materials in Civil Engineering*, 19(8), pp.683-690. Doi: 10.1061/(ASCE)0899-1561(2007)19:8(683)
39. Guldentops, G., Nejad, A.M., Vuye, C. and Rahbar, 2015. N., "Performance of a pavement solar energy collector: Model development and validation". *Applied Energy*, 163, pp.180-189. Doi: 10.1016/j.apenergy.2015.11.010
40. Kline, S.J., 1985. "The purpose of uncertainty analysis". *Journal of Fluids Engineering*, 107, pp.163-163.

#### COPYRIGHTS

©2021 The author(s). This is an open access article distributed under the terms of the Creative Commons Attribution (CC BY 4.0), which permits unrestricted use, distribution, and reproduction in any medium, as long as the original authors and source are cited. No permission is required from the authors or the publishers.



## Persian Abstract

## چکیده

سطوح آسفالت دارای ضریب جذب بالایی هستند و به جهت اینکه در طول روز در معرض تابش طولانی مدت آفتاب قرار می‌گیرند، دمای این سطوح تا نزدیک  $80^{\circ}\text{C}$  بالا می‌رود. از اینرو سطوح آسفالت به راحتی امکان تبدیل شدن به گرمکن خورشیدی هوا را دارا می‌باشند. از طرفی آسفالت دارای دلیل ضریب هدایت حرارتی پایینی است که این امر سبب انتقال حرارت جابجایی ضعیف بین سطح آسفالت و هوای عبوری از روی آن می‌شود. در این مطالعه تجربی استفاده از براده‌های آلومینیوم به عنوان پوشش سطح آسفالت جهت بهبود کارایی کلکتور هوایی آسفالت بررسی می‌شود. برای این منظور، یک گرمکن هوایی مارپیچ ساخته شده و از تعدادی حسگر به منظور بررسی و مشاهده رفتار دینامیکی این گرمکن و شرایط محیطی پیرامون استفاده شده است. برای بهبود انتقال حرارت بین هوای عبوری با سطح آسفالت و افزایش زبری سطح آسفالت از براده‌های آلومینیوم مشکی رنگ به عنوان پوشش سطح جاذب بهره برده شده است. برای مطالعه رفتار دینامیکی گرمکن هوایی، دو سناریو شامل گرمکن هوایی با سطح جاذب بدون پوشش و گرمکن هوایی با سطح جاذب پوشش داده شده با  $0.2$  کیلوگرم براده آلومینیوم در نظر گرفته شده است. مطالعه تجربی در شرایط محیطی و با دو دبی جرمی  $0.2$  و  $0.3$  کیلوگرم بر ثانیه انجام پذیرفته است. بر اساس نتایج مطالعه تجربی، گرمکن هوایی با سطح جاذب پوشش داده شده، هوای خروجی با دمای بالاتر، نزدیک  $5^{\circ}\text{C}$  الی  $9^{\circ}\text{C}$  در دبی‌های جرمی  $0.2$  و  $0.3$  کیلوگرم بر ثانیه تولید می‌کند. همچنین دمای سطح جاذب پوشش داده شده با براده‌های آلومینیوم به مقدار  $4^{\circ}\text{C}$  الی  $5^{\circ}\text{C}$  از سطح جاذب مشابه بدون پوشش بالاتر است. از این‌رو، استفاده از رویکرد پوشش سطح جاذب راندمان حرارتی گرمکن هوایی را به مقدار  $12/5$  و  $44\%$  به ترتیب در دو دبی جرمی  $0.2$  و  $0.3$  کیلوگرم بر ثانیه افزایش می‌دهد.